STRAIN CAPABILITY OF OPTICAL FIBRE BRAGG GRATING SENSING IN COMPOSITE SMART STRUCTURES

C Y Wei [1], S W James [2], C C Ye [2], N D Dykes[1] R P Tatam [2], and P E Irving[1]

[1] *Damage Tolerance Group, School of Industrial and Manufacturing Science*
[2] *Optical Sensors Group, Centre for Photonics and Optical Eng., School of Mech. Eng.*
Cranfield University, Cranfield, Bedford MK43 0AL, UK

SUMMARY: This paper determines the performance of Fibre Bragg Grating (FBG) sensors for strain sensing applications in carbon fibre composite materials. Carbon fibre laminates in either cross-plied or quasi-isotropic stacking sequences were fabricated using T300/Hexcel 914 prepregs. The FBG optical sensors were either surface attached, or embedded within the laminates. The sensor orientation was aligned either parallel or transverse to the adjacent carbon fibre layers. The sensor was also bonded to the surface of an aluminium plate using a high failure strain adhesive to allow the maximum failure strain of the sensor to be determined. The composite structures with integrated FBG sensors were subjected to static tensile loading. A scanning fibre Fabry-Pérot filter was used to monitor the reflected Bragg wavelengths. The optical sensor embedded between two 90° carbon fibre plies shows a high sensitivity to multi-site cracking formed in the transverse plies. The embedding in 90° plies seems to change the local stress distributions and to become a source of crack initiation. Efficient stress transfer from the host materials to the sensors is dependent upon incorporation methods, the thickness of the adhesive layers, and the location of the sensors.

KEYWORDS: Fibre Bragg grating sensor, Strain sensor, Smart materials

INTRODUCTION

The potential for the use of optical fibres as sensing elements in smart materials structures has resulted in considerable interest from the civil [1] and aerospace engineering communities [2] over the past decade. Fibre Bragg grating (FBG) sensors appear to offer a real prospect for widespread implementation, as they have wavelength-based sensing, offer single ended connection to control systems and exhibit a linear relation between applied strain and reflected wavelength [3]. A FBG consists of a periodic modulation of the refractive index of the core of an optical fibre, produced by exposure of the fibre to a structured UV laser beam. The FBG is a distributed Bragg reflector, acting as a narrow-band spectral channel-dropping filter in transmission, and as a narrow band reflection filter. The centre wavelength of the reflection band is dependent upon the period of the index modulation, which is sensitive to the strain and temperature experienced by the local region of the fibre. All other wavelengths outside the reflected band are transmitted.

The physical features of optical fibres, (size, mass, and thermal coefficient etc), allow them to be integrated into fibre composites during processing. The embedding has been shown to have minimal effects upon the stiffness, tensile and shear strength of the materials, although the compressive strength appears to be compromised [4-6]. Surface attachment of the optical fibre

sensors to structures is attractive for a wide-range of application areas (e.g. bridges or aero-structures) as no modification has to be made to the manufacturing process, and the sensor can be retro-fitted to any existing structures. However, for either embedment or surface attachment, a reliable incorporation method is required to guarantee an effective stress transfer from the host material or structure to the fibre sensor. Stress transfer is dependent on a combination of various factors: fibre coating types and thickness [7], the interface between the matrix and coating, or between coating and sensors, and orientation with respect to the neighbouring fibre layers. Because a resin rich region is formed if the direction of the optical fibre is transverse to the neighbouring reinforcements, which can be a potential weakness in the structure, attention has been paid to minimise the intrusive effects [8]. However, the strain sensing performance of FBGs is not well characterised when the orientation of the optical fibre is parallel or transverse to neighbouring layers. Relatively little attention has been paid to the sensitivity to multi-site cracking formed in carbon fibre laminates. Sensor durability and fidelity in structural monitoring are also a major concern. Knowledge of these factors is important as it allows a full exploitation of their potential for applications in smart materials and structures.

FBG SENSOR FABRICATION AND STRAIN SENSING DEMODULATION

FBGs with a length of 3 - 4 mm, with a Bragg wavelength of 1300 nm were fabricated in commercially available photosensitive Ge-B co-doped optical fibre (Fibrecore 1250). Prior to UV exposure, a 15 mm length of the protective polyacrylate coating, which has a high absorption in the UV, was removed chemically. The FBGs were written using the phase mask technique with UV irradiation at 266 nm.

The formation of the FBGs, and their response to loading was monitored using the system shown in Figure 1. The output from a fibre pigtailed broadband superluiminescent diode operating at 1300 nm with an optical bandwidth of 40 nm was used to address the FBG. The reflected signal, after passing through a scanning fibre Fabry-Pérot tuneable filter was monitored on an avalanche photodiode. The Fabry-Pérot had a free spectral range of 50 nm, and finesse of 220. The Fabry-Pérot filter could be locked to the spectral peak returned from FBG and the error signal used to monitor changes in the Bragg wavelength induced by loading.

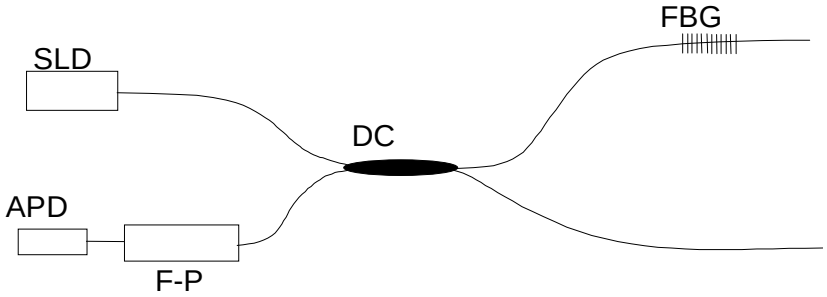

Fig. 1: Schematic of strain demodulation system
SLD: superluminescent diode, DC: directional coupler, FBG: fibre Bragg grating, F-P: scanning fibre Fabry-Pérot tuneable filter, APD: avalanche photodiode

The reflected wavelength, λ_B, from a FBG is determined by the effective refractive index of the propagating fibre mode, n_{eff}, and the grating period, Λ, from the expression:

$$\lambda_b = 2n_{eff}\Lambda \quad (1)$$

From Eqn 1, any changes in either n_{eff} or Λ will lead to a shift in the reflected Bragg wavelength. The shift in Bragg wavelength induced by an applied strain can be expressed as [9]:

$$\frac{\Delta\lambda}{\lambda_0} = (1 - P_{eff})\varepsilon_x \tag{2}$$

where $\Delta\lambda$ is the wavelength shift induced by the strain, ε_x, λ_0 is the reflected Bragg wavelength at zero applied strain and P_{eff} is the effective strain-optic coefficient. For germanosilicate glass, P_{eff} has a theoretical value of 0.22 [10].

MATERIALS DESIGN AND MECHANICAL TESTING

Optical fibres containing FBGs were incorporated into composite structures using both surface mounting and embedding methods. The carbon fibre laminates were fabricated from T300/Hexcel 914 prepregs. Lay-up sequences were designed to be orthogonal (OG): $(90°_2/0°_2)_{2s}$; and quasi-isotropic (QI): $(0°_2/45°_2/90°_2/-45°_2)_s$

In the tensile testing procedures, the 0° plies are defined as the layers containing carbon fibres laid parallel to the stress direction. The optical fibres were oriented such that they laid either parallel or transverse to the adjacent carbon fibre orientation, but always aligned with the tensile stress direction. The test coupons containing FBG sensors were designed and fabricated in a variety ways as listed in Table 1.

Table 1. Orientation of the optical fibres with respect to ply lay-up

Host materials	Incorporation methods	Sensor position and orientation
OG	Surface mounting	Transverse to the surface carbon fibres
OG	Embedding	Between two 90° plies $(90°/FBG/90°/0°_2/90°_2/0°_2)_s$
OG	Embedding	Between 90° and 0° plies $(90°_2/FBG/0°_2/90°_2/0°_2)_s$
QI	Embedding	Between 0° $(0°/FBG/0°/45°_2/90°_2/-45°_2)_s$
Aluminium (Al7075)	Surface mounting	Parallel to 0°

Figure 2 shows schematically how the sensors were incorporated into the OG laminates via either surface mounting or embedding methods. To fabricate the laminates with embedded sensors, the optical fibres containing one FBG were laid during hand lay-up of the T300/914 prepregs. The sections of the optical fibres which entered and exited the laminates were protected by a plastic tube to avoid crush damage which could occur during curing in an autoclave. After curing, the laminates had a thickness of 2.24 mm. Araldite 5052 (a room temperature curing adhesive) was used to mount the optical fibre containing FBGs on the surface of the carbon fibre laminates.

The specimens used for tensile testing were 300 mm long, and 30 mm wide. The test coupons were clamped by two pairs of special designed clamps, which ensure that the tensile failure occurred within the 180 mm gauge length. The tests were conducted under displacement control mode. The loading rate was maintained at 0.25 mm/min. The temperature in the test lab was monitored during the mechanical testing. A maximum variation of ±1° was determined. Tensile stress was calculated by dividing the applied load by the cross-section area of the specimens. For all the mechanical tests, a conventional electrical strain gauge (E-gauge), attached to the surface of the test coupons close to the location of the FBGs, was used as a reference strain measurement for calibration and comparison of results. The sensing length of the strain gauges was 5 mm. During all the mechanical tests, the strain induced shift of the reflected Bragg wavelength was accurately measured using a Fabry-Pérot tuneable filter, from which a strain resolution of the order of 1με could be achieved. Aluminium plates (Al 7075), with FBGs bonded to the surface using an epoxy/polyurethane blend adhesive, were subjected to static tensile stress to determine the maximum failure strain of the FBGs.

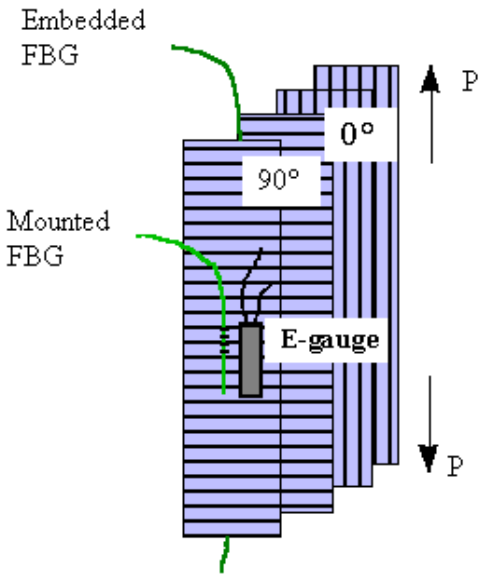

Fig. 2: Schematic showing arrangement of FBG sensors either surface mounted on the 90° fibre surface or embedded between two 90° plies in an OG laminate. The strain gauge position and loading direction are also shown.

A scanning electron microscope (SEM) was used to observe the structure of optical fibres which were integrated between either 0° or 90° carbon fibre plies. The specimen containing the optical fibre embedded between 90° plies was subjected to an ultrasonic C-scan to determine the crack spacing in the 90° layers after tensile loading.

RESULTS AND DISCUSSION

Under all test circumstances, the Bragg wavelength was monitored using the Fabry-pérot interrogation system. The strain of FBG sensors was determined from the wavelength by applying Eqn. 2. The strain measured from the strain gauge was also presented as a reference to compare measurement results from the optical sensors.

Strain sensing range

Epoxy/polyurethane blend compounds, which were used as the adhesive to attach the optical fibre to the aluminium plate, have a failure strain above 5%. The large failure strain ensured that no cracks or debonding occurred before the failure of the optical fibre, allowing the maximum strain range of the sensor to be determined.

Figure 3 shows the curve of strain against stress of Al7075 obtained both by the FBG and strain gauges. The tensile stress-strain curves produced by the FBG and electrical strain gauges are overlapped in most of the sections, showing a close agreement within the linear elastic region (< 0.6%). However, a maximum discrepancy up to 4 % was observed in the large strain region (> 2%). This discrepancy increased with increasing strain. The strain obtained from the FBG sensors is higher than that measured via the strain gauge. Without any third method to determine the strain, it is impossible to state which value is more accurate. Although the FBG sensor is also sensitive to the change of environmental temperatures, during the tests, a maximum ±1°C change of temperature was monitored, which induces ±11 με variation to the strain reading. This error may be responsible for only 0.1% discrepancy. The causes of the rest 3.9% discrepancy remain unclear. This will be further investigated by employing alternative strain measurement methods. The optical fibre fractured when the strain reached 22,000 με. The failure strain of pristine optical fibres, measured before stripping and UV irradiation process can be as high as 6.3 %. The failure strain of an optical fibre containing a FBG can be limited by the reduction in the strength of the fibre caused by the FBG fabrication process [11].

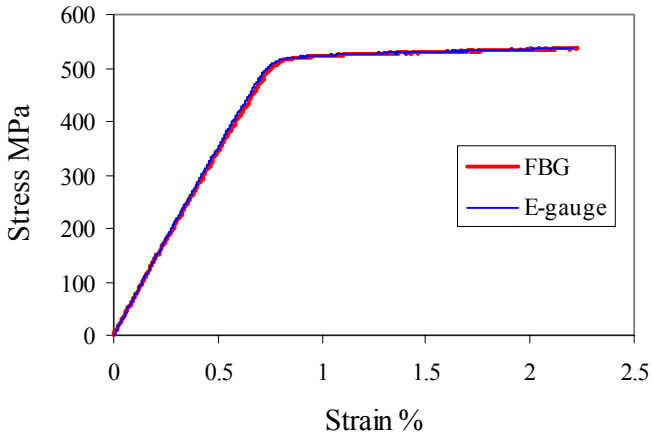

Fig. 3: Tensile strain of aluminium plate determined by both strain gauge and FBG sensor

FBGs incorporated adjacent to 0° carbon fibres

The strain measured by a surface attached FBG laid along the carbon fibre direction is plotted against loading-time in Fig. 4, which also includes the measurements provided by a strain gauge. The strain measured by the two techniques follows the trend of the stress applied to the QI laminate. In the high strain range (above 0.8%), the strain measured by the FBG has a slightly lower value than that measured by the E-gauge. The maximum discrepancy is 150 με when the strain reaches to the maximum value of 12, 000 με. This might be a result of a lag in the stress transfer from the host materials to the sensor through the adhesive layer at these high stress levels. The principle of the stress transfer from host materials to optical sensors is

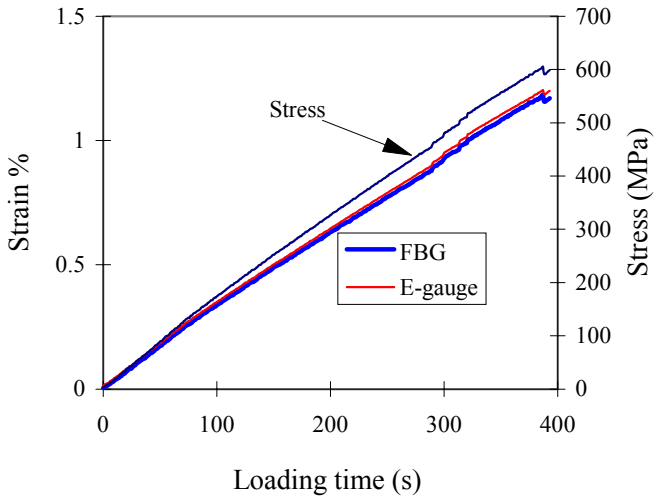

Fig. 4: Strain measured by a strain gauge and a FBG sensor which was attached on the 0° fibre surface of a QI laminate

illustarted in Figure 5. The adhesive has a much lower elastic modulus (about 2 GPa) than optical fibres (79 GPa) and the QI laminate (49 GPa). The deformation can be very significant if the thickness of the adhesive layer is large. A thin adhesive layer is expected to allow accurate strain monitoring of smart structures by surface attachment.

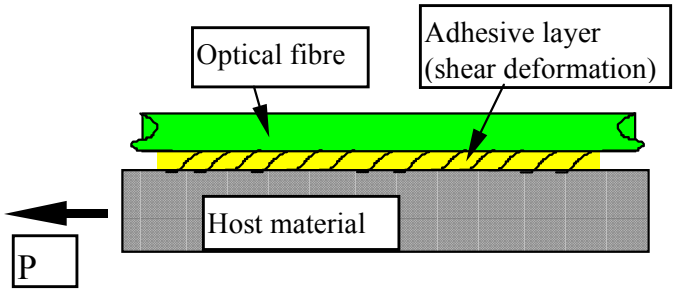

Fig. 5: Diagram showing the stress transfer from host materials
to optical fibre sensor through adhesives

Figure 7 shows the strain measured by a FBG sensor embedded between two 0° carbon fibre plies in a QI laminate. Similar to the surfaced attached FBG, the strains obtained from both strain gauge and FBG sensors follow each other in up to 0.8% strain.

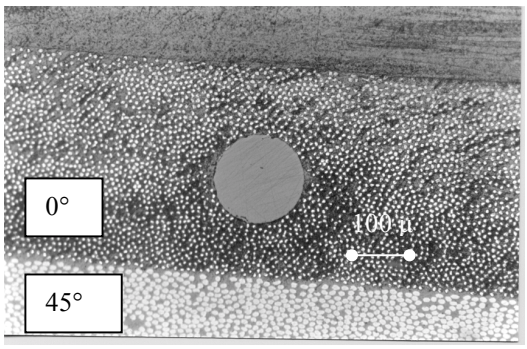

Fig 6: SEM photo showing
the configuration of
an optical fibre without coating
(with a diameter of 125 µm)
embedded in 0° plies

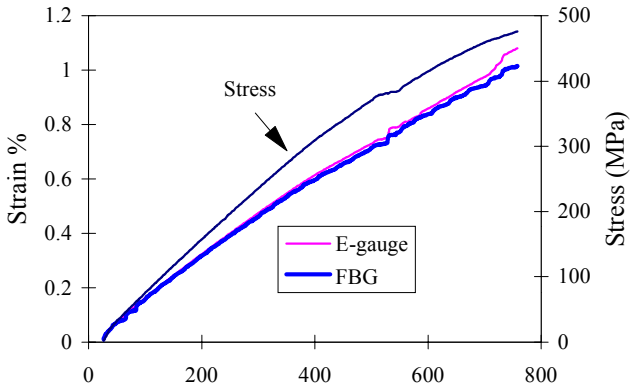

Fig. 7: Strain measured from a strain gauge
and a FBG sensor embedded between 0 ° plies
in a QI laminate

The discrepancy between the readings then increases. The FBG measurement is slightly lower than the strain gauge value and the FBG strain curve shows a few small steps after the strain reached 0.8%. These discontinuities in the response of the FBG may be attributed to the cracks formed at the 45 ° fibre layer which is only one ply beneath of the FBG sensor. Figure 6 shows the structure of the coupon produced by this orientation of the optical fibre. The FBG sensor may sense the cracks in the 45° layer that are located about 70 µm away from the sensor. The optical fibre is intimately surrounded by carbon fibres in this 0° embedding. The stress transfer from the surroundings to the FBG sensor can be expected as the best way to record the 0° strain of the laminate. Cracking occurred at 45° appears to change the stress transfer function which leads to the discrepancy of the strains between the strain gauge and FBG sensors.

FBGs incorporated adjacent to 90° carbon fibres

When testing a coupon in which the FBG and the electric strain gauge were oriented transverse to the surface carbon fibre direction, as shown in Fig. 2, a difference of strain response to the 90° cracking was observed in the stress-strain curves plotted in Fig. 8. The FBG sensor appears very sensitive to the cracking occurring in the 90° layers, as indicated by many discontinuities in the curve. The internal structure of the coupon produced by embedding the optical fibre into 90° plies is shown in Fig. 9. Because the optical fibre is transverse to the adjacent carbon fibres, this embedding creates a 'resin eye', which has a length of 1.25 mm.

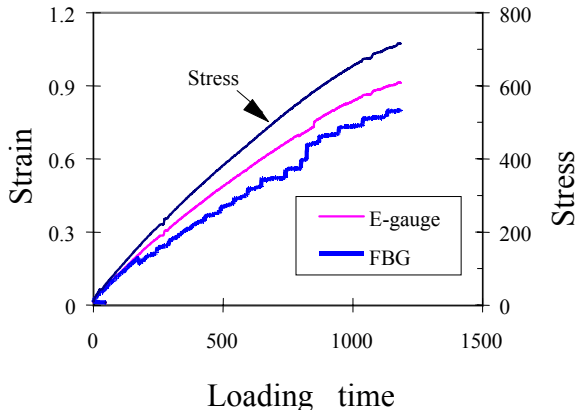

Fig. 8: Strain measured by a strain gauge and FBG sensor which was embedded between 90° plies of an OG laminate

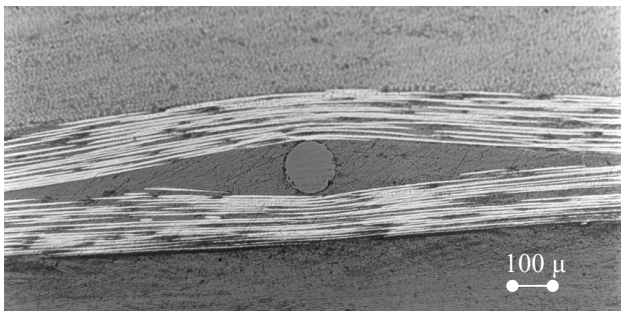

Fig. 9: SEM photo showing the optical fibre embedded transversely to the carbon fibre direction forming a 'resin eye' as long as 1.25 mm

The cross-section of the optical fibre shown in Fig. 9 was within the sensing region, in which the polyacrylate coating was removed. The bare fibre length is around 15 mm and has a diameter of 125 µm. This size is 25 times the size of a single carbon fibre (~5 µm). The intrusion of the optical fibre forms stress concentration sources. In addition to the presence of the 'resin eyes', the embedded optical fibre is located at transverse crack centres as shown in Fig. 10. In this c-scan image, cracks around the optical fibre are clearly observed. Interestingly, no cracks existed within the 15 mm stripped section, but one crack formed at each end of the section, where the presence of the polyacrylate coating increases the diameter of the fibre to 250 µm. Using this information, the sensing performance of the FBG in Fig. 8 might be explained. At an applied strain of 0.2%, there is an obvious discontinuity in the curve and the line begins to deviate from the strain line output from the E-gauge. However, the strain of the FBG sensor continues to increase with a series of discontinuities. The first discontinuity may be a result of the formation of the two cracks at the ends of the bare fibre section, which caused partial debonding of the sensor from the matrix of the composite. The tensile stress was then not fully transferred from the host material to the sensor. Other sections of the optical fibre were still bonded with the laminate. However, as the test proceeded, the increasing stress continuously created cracks at the transverse layer. The formation of the cracks is accompanied by a release of stress energy. The extra strain induced by the formation of each crack was sensed through the stress transfer from the non-sensing parts of the fibre to the FBG, producing a step in the strain curve. It is assumed that the step height may be related to the crack width. The crack

spacing determined by the c-scan shown in Fig. 10 is around 4 mm. The cracks are quite evenly distributed. A crack density saturation (defined as the Characteristic Damage State - CDS) has been reported with the cracks in the off-axis plies [12]. The cracks are formed at regularly spaced intervals. The CDS is independent of load history, initial stress, but dependent of stacking sequence and lamina properties.

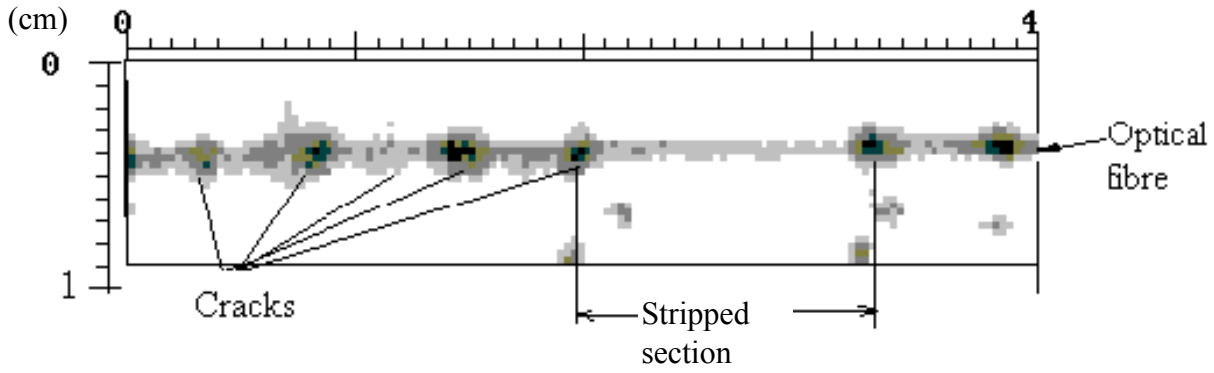

Fig. 10 C-scan image after tensile testing of the FBG sensor which was embedded between 90° plies

For surface mounted optical fibres, attached transversely to the surface carbon fibre orientation, the strain determined from the FBG sensor is plotted in Fig. 11. Unlike the embedded situation, no interruption in the composite structure exists with the surface mounting method. Optical fibres will not be the sources of crack initiation. The sensing performance of the FBG in Fig. 11 shows a number of differences from those in Fig 8. In this case the strain is observed to decrease when cracks are formed in the transverse plies. The formation of the cracks caused the adhesive layer to debond from the laminate surface. The stress that the host laminate was subject was not effectively transferred to the optical sensor through the adhesive layer. The debonding reduced the stress of the optical fibre, which results in a decrease in strain. Unlike the embedded optical fibre, the surface attached fibre is located at the tip of the cracks in the 90° layer. The crack formation does not have a direct impact on the optical fibre as it does for the fibre embedded inside the transverse plies. Consequently, not all crack formation is detected. A step increase in the strain measured by strain gauges similarly appears around 0.7% in both Fig. 8 and Fig. 11, which corresponds to a modulus reduction induced by 90° cracking. This may suggest that the transverse embeddment has little effect on global mechanical properties, but significantly changes the local stress distribution and influences the formation of transverse cracks.

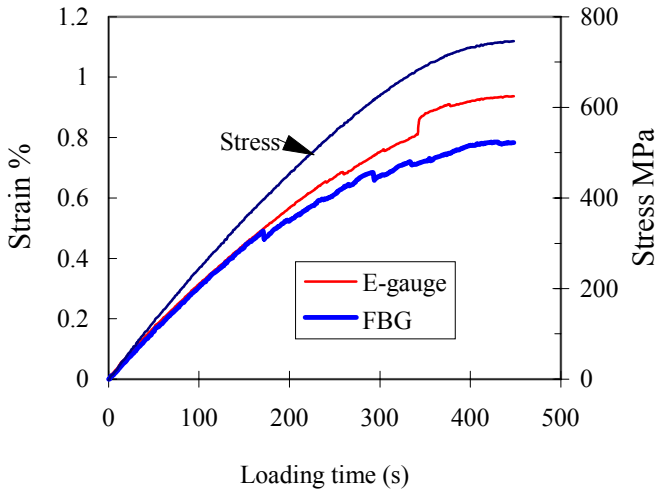

Fig. 11: Strain measured by a strain gauge and FBG sensor which was surface mounted on the 90° fibre surface of a cross-plied laminate

CONCLUSIONS

The fidelity of the FBG strain measurement in a composite smart structure is greatly dependent on the effective transfer of strain from the host material to the optical fibre. The efficiency of strain transfer has been investigated for the two incorporation methods: surface mounting and embedding. This work has shown that many factors can influence the efficiency of strain transfer. The following conclusions are reached:

1) In the surface mounting method, the thickness of the adhesive layer and the elastic properties are critical for high fidelity measurements.
2) The current sensor fabrication method offers the sensor failure strain of 22, 000 με. The strain range can be enhanced by improving the fabrication procedure.
3) The embedding of optical fibres between two 90° plies shows the capability of sensing the formation of transverse cracks, which may be beneficial in specialist applications.
4) The transverse embeddment has little effect on global mechanical properties, although it significantly changes the local stress distribution and influences the formation of transverse cracks.
5) Post-test non-destructive tests show that cracks are associated with the regions of the fibre having polyacrylate coating. No cracks were detected around the stripped region of the fibre.
6) This investigation has demonstrated that FBG sensing successfully monitors cracking of carbon fibre composites in both surface mounting or embedding methods.

ACKNOWLEGMENTS

AEA Technology Plc and British Civil Aviation Authority (CAA) are gratefully acknowledged for sponsoring this project. Thanks are due to Dr K Winters and Dr R Davidson from AEA and Dr J Bristow from CAA for many useful discussions.

REFERENCES

1. Fuhr, P.L., and Huston, D. R., 'Intelligent Civil Structures Efforts in Vermont-An Overview', *Smart Sensing, Processing and Instrumentation*, SPIE vol 1918, New Mexico, 1993, pp. 412-419.
2. Van Way, C.B., and Kudva, J. N., et al, 'Aircraft Structure Health Monitoring System Development-Overview of the Air Force/Navy Smart Metallic Structures Program', *Smart Structures and Integrated Systems*, SPIE vol 2443, San Diego, 1995, pp. 277-285.
3. Measures, R. M., Alavie, T., Karr, S., and Coroy, T., 'Smart Structure Interface Issues and Their Resolution: Bragg Grating Laser Sensors and the Optical Synapse', *Smart Sensing, Processing and Instrumentation*, SPIE vol 1918, New Mexico, 1993, pp. 256-262.
4. Carman, G.P. and Sendeckyj, G. P., 'Review of the mechanics of embedded optical sensors', *J. Composites Technol. and Research*, 17, pp183-193 (1995).

5. Mall, A., Dosedel, S. B., and Holt, H.W., 'The performance of graphite epoxy composite with embedded optical fibers under compression', *Smart Mater.Struct.* 5, 1996, pp. 209-215.
6. Measures, R. M., 'Fiber optic composite smart structures', *Composite Eng.* **3**, pp715-750 (1993).
7. Madsen, J.S., and Jardin, A.P.,et al, 'Effect of Coating Characteristics on Strain Transfer in Embedded Fibre-optic Sensors', *Smart Sensing, Processing and Instrumentation*, SPIE vol 1918, New Mexico, 1993, pp. 228-236.
8. Culshaw, B., and Michie, W. C., 'Smart Structures-the Role of Fibre Optics', Interferometry'94: *Interferometric Fibre Sensing*, SPIE vol 2341, Poland, 1994, pp. 134-151.
9. Butter, C.D., and Hocker, G.P., 'Fiber Optics Strain Gauge', *Appl. Opt*. 17, pp. 2867-2869 (1978)
10. Morey, W.W., Meltz, G., and Glenn, W. H., 'Fibre Optic Bragg Grating Sensors', *Proc. Fibre Optic and Laser Sensors VII*, Boston, 1989, pp. 98-107
11. Wei, C.Y. and James, S.W., Ye, C.C. Tatam, R.P. and Irving, P.E., 'The Influence of Process Route on Mechanical and Sensing Performance of Fibre Bragg Grating Sensors', *Sensory Phenomena and Measurement Instrumentation for Smart Structures and Materials*, SPIE vol 3670, San Diego, 1999, Paper 3670-29
12. Reifsnider, K.L. and Highsmith, A., 'Characteristics Damage States: a New Approach to Representing Fatigue Damage in Composite Laminates'. *Proceedings of Fatigue'81*: Materials, Experimentation and Design in Fatigue. Warwick, 1981, pp. 246-260.